Simulation of Quenching Laminar Hydrogen-Air Flames in a Mesh Arrestor

H. Saitoh
Department of Engineering Science and Mechanics
Shibaura Institute of Technology, Tokyo 135-8548 JAPAN
hsaito@sic.shibaura-it.ac.jp

J. Melguizo-Gavilanes
Institut Pprime
UPR 3346, CNRS, ENSMA
University of Poitiers, Futuroscope-Chasseneuil, FRANCE
josue.melguizo-gavilanes@cnrs.pprime.fr

J.E. Shepherd
Graduate Aerospace Laboratories
California Institute of Technology, Pasadena CA 91125 USA
joseph.e.shepherd@caltech.edu

November 30, 2017

Abstract

Numerical simulation was used to investigate the quenching of laminar hydrogen-air flames by a fine-wire metal-mesh flame arrestor. The unsteady propagation of a flame through a periodic array of wires was investigated using the reactive Navier-Stokes equations with a detailed model of the chemical kinetics, realistic thermochemistry and models for diffusive transport. The geometry of the arrestor was a two-dimensional periodic array of wires 0.12 mm in diameter spaced between 0.1 and 0.5 mm apart and placed perpendicular to the plane of motion. Critical wire spacing for flame extinction was determined for three equivalence ratios, 0.4, 1.0 and 1.6. The Péclet number corresponding to the critical conditions is an increasing function of equivalence ratio, varying from 2.5 to 15 over the range examined. The process of flame interaction with the arrestor is visualized with temporal sequences of selected field variables and plots along the centerline at times before, during and after the interaction.

Keywords: Laminar flame, Hydrogen, Quenching, Arrestor, Simulation

1 Introduction

Flame arrestors are widely used in the chemical process and transportation industry [3] as a safety measure to prevent flames from propagating through piping systems or into vessels containing flammable gases. The principle of operation of most arrestors is to quench the flame and cool the following flow by introducing a large surface area of cold metal surrounding small flow passageways. If the gas flow emerging from the arrestor is sufficiently cold and deficient in reactive species, the flame will not be transmitted downstream.

One of the first and simplest arrestor designs is single or multiple layers of fine-wire mesh similar to that shown in Fig. 1. A recent application of mesh arrestors to explosion mitigation is discussed by **(author?)** [12]. Many other designs are in use today, such as a bundle of small diameter tubing, sintered metal plug, a crimped ribbon or a perforated plate [3]. The design and specification of flame arrestors are highly empirical and relies to a large extent on standardized testing [4]. On the other hand, the combustion community has for several decades been studying flame quenching as a scientific endeavor [1] to understand the source of pollutants due to incomplete or partial combustion in the near-wall region of combustion engines and combustion chambers.

The goal of the present study is to investigate the potential of numerical simulation for understanding the mechanisms of flame extinction in arrestors. Two-dimensional numerical simulations were performed to examine the interaction of a hydrogen-air laminar flame with a simplified model of a mesh flame arrestor. A detailed chemical kinetic mechanism for hydrogen was used to achieve high-resolution numerical simulations with a realistic treatment of the key physical and chemical processes and properties.

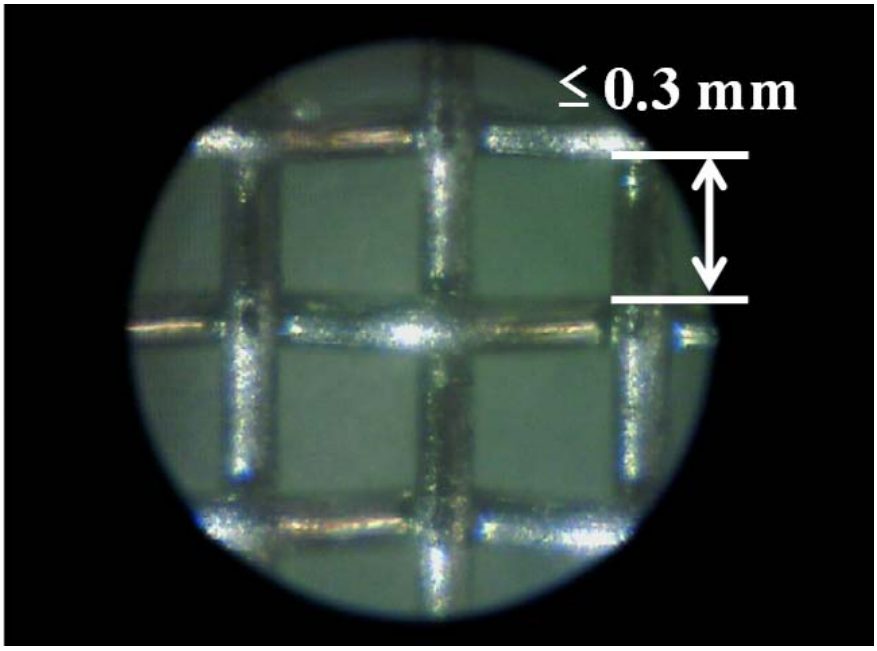

Figure 1: Typical wire mesh screen used in a flame arrestor.

2 Computational Approach

Our approach for this initial study is to consider only the reactive flow aspects of the arrestor performance, focusing on the interaction of the flame with a rigid, inert and cold wire mesh. Based on previous numerical and experimental studies [8, 5], heat transfer by conduction from the gas to the metal mesh is the expected dominant process that causes flame extinction; therefore, the current study models the transport of thermal energy within the gas with high fidelity. However, heat transfer within the mesh wires is not considered, the surface is treated as an isothermal heat sink with constant surface temperature, consistent with the previous studies at low pressure [8]. This simplification is possible because at atmospheric pressure the thermal conductivity k and heat capacity per unit volume ρC_p of the metal (stainless steel) are 2-3 orders of magnitude larger than that of the gas and the interaction time of interest is short, less than 500 μs. As a consequence, the peak surface temperature of the metal is estimated to increase less than 2 K and the thermal layer within the solid is smaller than the radius of the wire for the duration of the simulation.

In the present study, the heat transfer within the wire mesh is not a significant issue despite peak heat fluxes that exceed 1 MW/m^2 during the interaction with the flames and the following flow. At high pressures [8] or with repeated use within a short duration, heating of the arrestor has to be considered and is known to degrade the performance [3]. At higher surface temperatures, surface reactions may also need to be considered; however, at the low surface temperatures of the current study, surface reactions are not significant [8, 5].

In order to simulate the flame propagation and interaction with the wire mesh, we carried out time-accurate simulations resolving both the flame structure as well as the viscous and thermal boundary layers around the wires. The simulations were performed using the OpenFOAM [13] software with a solver for the low-Mach number approximation to the reactive Navier-Stokes equations. The details of the computational methodology, including the reaction mechanism [11], molecular transport approximations, spatial and temporal discretization and validation testing, are described in [10, 9].

The geometry of our arrestor model is the two-dimensional planar shape shown in Fig. 2 containing one cell of a periodic, two-dimensional analog of the wire mesh. The actual computational domain is the region enclosed by the dashed lines which consists of a rectangle with half-cylinder surfaces of diameter $d = 0.12$ mm simulating the wire in the arrestor mesh. The size and spacing of the cylinders is comparable to the actual flame arrestor used by Saitoh et al. [12]. The top and bottom boundaries of the domain are located

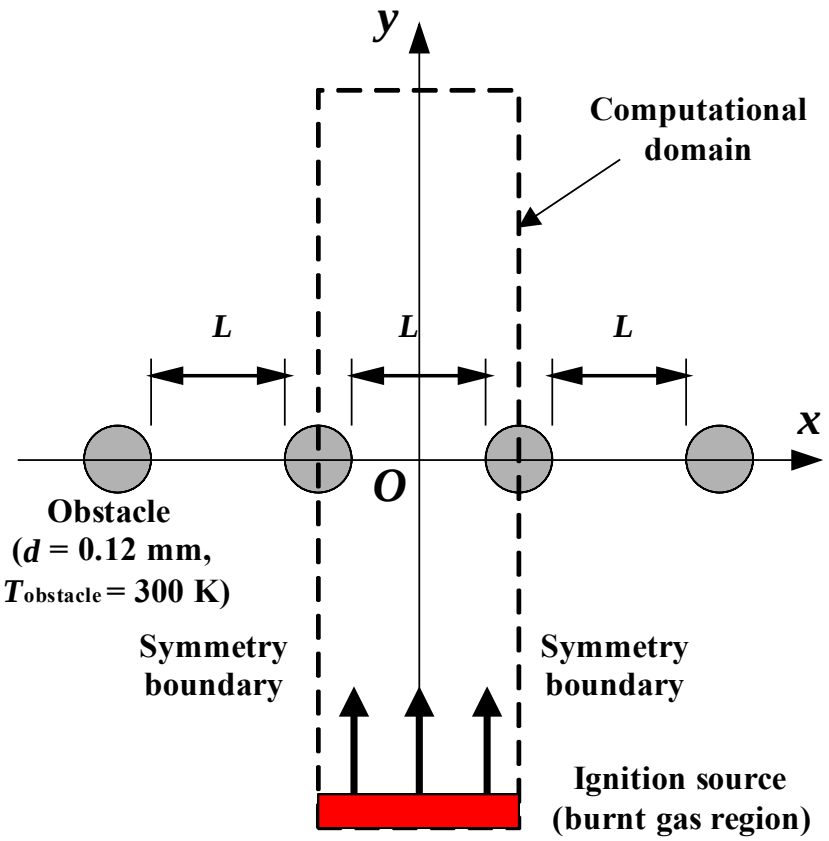

Figure 2: Computational domain used in simulations

10 thermal flame thicknesses above and below the cylinders.

The domain is discretized using 60,000 to 150,000 cells to obtain a resolution of at least 80 cells within the flame structure and a cell size of about 4 μm in the region adjacent to the obstacles. The grid conforms to the cylinders and gradually transforms to rectangular cells in the upstream and downstream regions. The boundary conditions on the cylinder surfaces are isothermal ($T_{obstacle}$ = 300 K), no slip, and zero net flux of species to the nonreactive surfaces. At the top of the domain, a non-reflective and pressure-transmissive boundary condition is used to simulate an outflow; at the bottom, all variables are set to zero gradient and the flow is forced to be symmetrical about the center line of the opening between the cylinders. The symmetry condition is equivalent to simulating the flow through an infinite array of cylinders in the x direction. The initial conditions are: P_0 = 101 kPa, T_0 = 300 K, and the domain is filled with hydrogen-air with a specified equivalence ratio Φ. The flame is initiated by imposing a region $2\delta_T$ in height of hot combustion products at the bottom boundary.

For each mixture, the thermal flame thickness δ_T and ideal laminar burning speed S_ℓ^o were computed in separate one-dimensional steady calculations using Cantera [2] and used to validate the values obtained from the two-dimensional simulations during the period of quasi-steady flame propagation upstream of the mesh. For Φ = 0.4, δ_T = 0.74 mm and S_ℓ^o = 0.175 m/s; for Φ = 1.0, δ_T = 0.37 mm and S_ℓ^o = 2.24 m/s; for Φ = 1.6, δ_T = 0.35 mm and S_ℓ^o = 3.06 m/s. The quenching model was validated against the classical parallel-plate quenching experiments used by Lewis and von Elbe [6] in their spark ignition tests. The computational geometry was an axi-symmetric region bounded at the top and bottom by planar, isothermal no-slip surfaces simulating plates perpendicular to the axis of symmetry. A cylindrical flame was initiated along the axis of symmetry by starting the simulation with a column of hot products of a specified radius. If the initial column radius was greater than the flame thickness, and the spacing between the plates was

larger than the quenching distance, then a flame propagating radially outward was created. Repeating the simulation and decreasing the plate spacing, a critical spacing was identified where the flame slows down and extinguishes. For a stoichiometric hydrogen-air mixture, a critical plate spacing of 0.4 to 0.5 mm was obtained as compared to the measured value of 0.64 mm; for a rich mixture, $\Phi = 1.6$, a critical spacing of 0.7 to 0.8 mm was obtained as compared to the measured value of 0.76 mm.

3 Results and Discussion

A series of simulations with varying mesh spacing L were carried out for a lean $\Phi = 0.4$, stoichiometric $\Phi = 1.0$, and rich $\Phi = 1.6$ mixtures in order to bracket the critical values L^* for extinction. Multiple simulations were performed to test the sensitivity of the results to grid refinement, domain height and transport model assumptions. The final computations used the mixture-averaged binary diffusion coefficients for mass transport rather than the more computationally inexpensive but less accurate constant, non-unity Lewis number model used in some previous studies [9]. The results of the final simulations are shown as discrete points corresponding to the outcome of either extinction (open symbols) or propagation (closed) of the flame downstream of the wire mesh. Near the critical condition, it is important to perform the simulation for a sufficiently long duration to ensure that the combustion products (particularly radical species such as OH) convected downstream of the mesh do not result in a delayed ignition. As discussed below, for near-critical cases, $L \approx L^*$, a distinct flame front is not observed after the flame passes through the mesh but an extended region of hot products with a pool of radicals can be observed for some distance downstream. Depending on the extent of the thermal boundary layer created by the heat conduction to the mesh, the radical pool will either decay or increase with time due to the competition between reaction, diffusion and convection. This process can take some time to play out for near-critical situations.

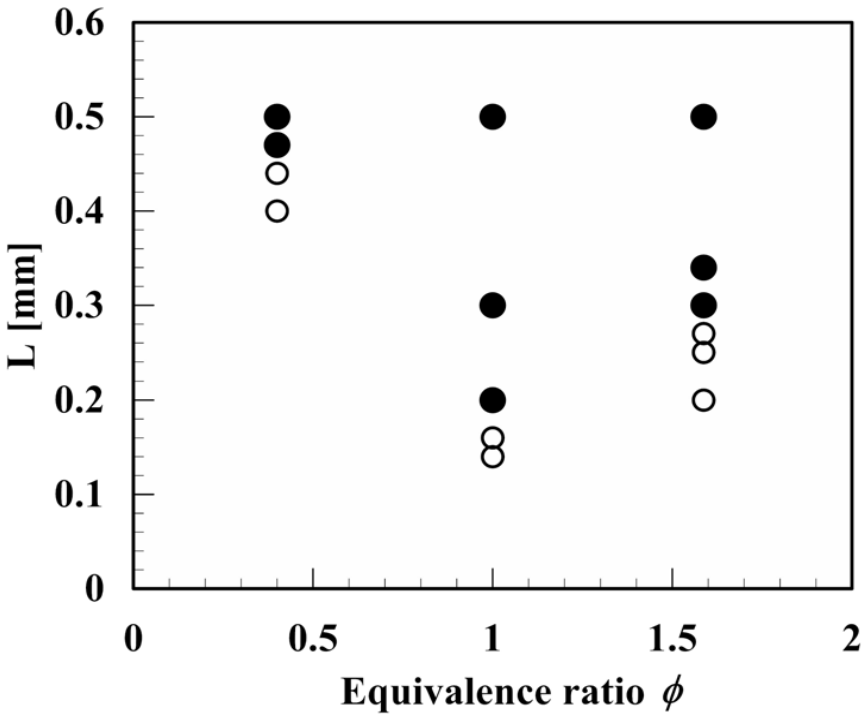

Figure 3: Results of simulations varying the mesh spacing L. Filled symbols - flame transmission; open symbols - extinction.

The critical mesh spacing L^* has a value of 0.16 mm for the stoichiometric case ($L^* = 0.44$ mm for $\Phi = 0.4$ and $L^* = 0.27$ mm for $\Phi = 1.6$). The $\Phi = 1$ value is significantly smaller than the Lewis and von

Elbe [6] critical parallel plate spacing value of 0.6 mm. This can attributed to the vastly larger extent of the quenching surface, a 25.4 mm diameter disk, in the parallel plate test as compared to the 0.12 mm diameter wires in the mesh arrestor. A much more effective flame arrestor than a mesh is a crimped metal ribbon [7]; for stoichiometric hydrogen-air the critical ribbon spacing for extinction is 0.3 mm. The disparity in critical spacing for flame extinction illustrates one of the key difficulties in developing predictive models for engineering flame arrestors, critical parameters are highly configuration dependent [3] and "quenching distances" are meaningful only in the context of a specific test setup and application. The increase in the critical mesh spacing for off-stoichiometric (rich or lean) mixtures observed in the present simulations is consistent with previous studies on flame arrestors and quenching tests.

An important parameter in determining critical flame arrestor dimensions is the flow velocity induced ahead of the flame, higher speeds increase the heat transfer rate to the wires but reduce the time that the active flame region is affected by heat transfer to the wires. In the $\Phi = 1$ case, the boundary conditions create flow speeds which are of the order 14 m/s in the reactants ahead of the flame and upstream of the mesh with a small dependence on L. The flow velocity on the centerline increases to peak values up to 35 m/s between the cylinders of the mesh due to the reduction in flow area in the $L = 0.14$ mm case. The characteristic Reynolds number based on wire diameter d for the unburned gas $Re_d = \rho V d/\mu$ is of the order 78; for considering heat transfer to the mesh, it is more appropriate to evaluate the viscosity μ and density ρ at the peak temperature in the flame, this reduces Re_d to 2.4. These values of Re and the flow velocities confirm that the numerical solution method we have chosen is appropriate and the flow regime through the mesh is laminar.

3.1 Flow Regimes

The evolution of the OH mass fraction, velocity magnitude and temperature fields are shown for three cases in Figs. 4, 5 and 6. These cases are taken from the study carried out with stoichiometric mixtures ($\Phi = 1$) to bracket the critical mesh spacing. Each figure presents a temporal sequence for each field variable at the times specified in the caption. These times cover the range from just before the flame reaches the wire mesh until after the event is concluded by either extinction or development of a flame downstream. These cases are representative of the generic regimes of behavior observed in all of the simulations carried out for this study.

3.1.1 Sub-critical case

This case has $L = 0.14$ mm $< L^* = 0.16$ mm. The outcome of this case is quenching of the flame immediately upon passing through the wire mesh (Fig. 4b) and although products can be observed downstream of the mesh in subsequent frames (Fig. 4c-d) of the temperature visualization, the peak temperature has been decreased to values substantially less than 1000 K, drastically decreasing the concentration of the radical species and interrupting the chain-branching process permanently so that the flame is quenched.

3.1.2 Near-critical case

This case has $L = 0.2$ mm $> L^*$. The outcome is the initial extinction of the flame passing through the wire mesh (Fig. 5b) and the temperature decreases to about 1500 K in the products downstream of the mesh. The initial extinction event is followed by a dwell period (Fig. 5c-f) during which the radical pool continues to grow, a significant amount of OH is visible in Fig. 5g, continued growth of the radical pool eventually leads to a coupled chain-branching/energy release process and a flame being re-established (Fig. 5h).

3.1.3 Super-critical case

This case has $L = 0.5$mm $>> L^*$. The opening between the wire is sufficiently large that the heat losses to the wire do not penetrate the centerline of the flow. The outcome is that despite partial quenching of the flame upon passing through the wire mesh (Fig. 6b), the chain-branching process continues in a high-temperature region within and immediately downstream of the mesh (Fig. 6c,d) and a propagating flame is reestablished across the entire domain (Fig. 6e,f). The distortion in the flame geometry observed in Fig. 6f is the combined

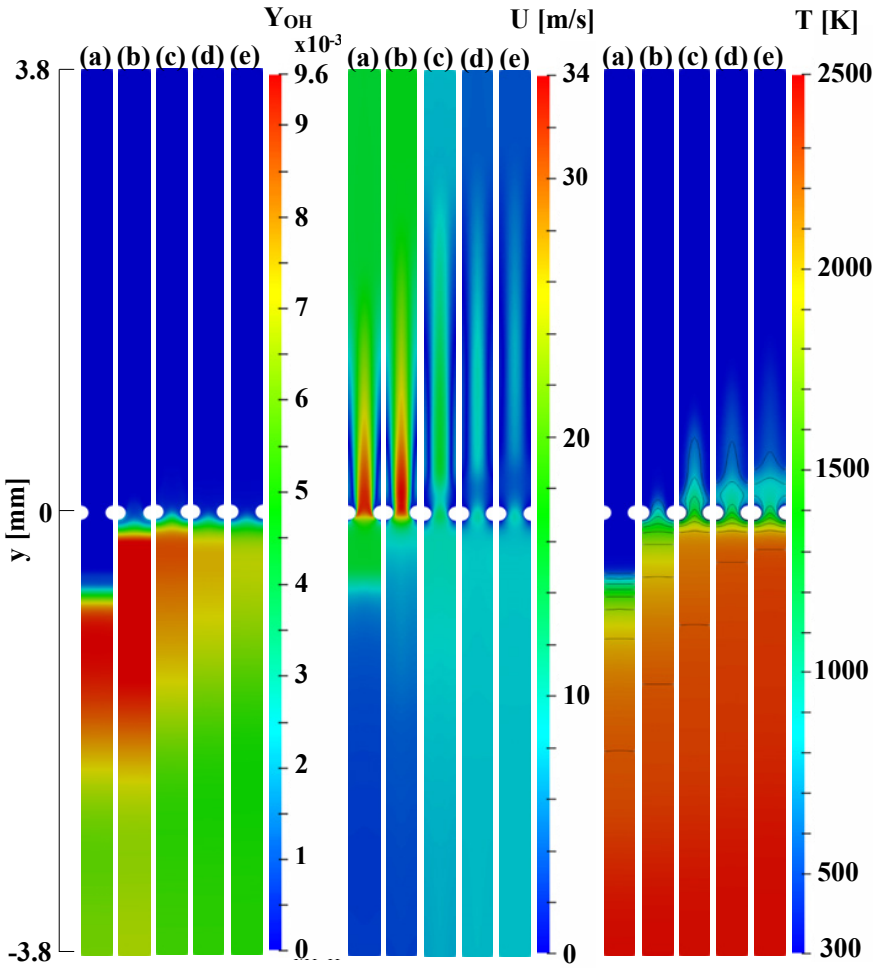

Figure 4: Sub-critical case, mesh spacing $L = 0.14$ mm. Times relative to flame arrival at the wire location are a) -30 μs, b) 0 μs, c) +30 μs, d) +60 μs, e) +90 μs.

effect of the quenching in the thermal boundary layer adjacent to the wires and the two-dimensional flow created by the mesh.

Temperature and selected species (H, O, OH, HO_2 and H_2O_2) mass fraction profiles on the centerline (Fig. 7) for the $\Phi = 1$ mixture further illustrate how the heat transfer to the wire mesh affects this pool of species for each of three cases. These species are crucial for the propagation of the chain-branching process leading to energy release by recombination that increases the temperature and accelerates the reactions, the process which is essential to maintaining flame propagation. Upstream of the wire mesh, the characteristic structure of a propagating flame with HO_2 and H_2O_2 visible in the low temperature region, followed by consumption of these species and a rapid rise in H, O and OH to peak values and subsequent approach to equilibrium with increasing temperature due to recombination. In the sub-critical case, the temperature drops to less than 1000 K immediately downstream of the mesh and continues to decrease with increasing distance. More significantly, the chain carrier H atoms drop to very low levels, breaking the branching chain processes and extinguishing the flame. In the near critical case, the temperature drops downstream but reaches a plateau, enabling the H atom concentration to remain at significant levels and ultimately continue the chain propagation process, leading to a re-establishment of the flame downstream of the mesh. In the supercritical case, the flame structure on the centerline is essentially unaffected by the heat transfer to the wires and propagates directly through the opening between the wire with no decrease in temperature or H atom concentration.

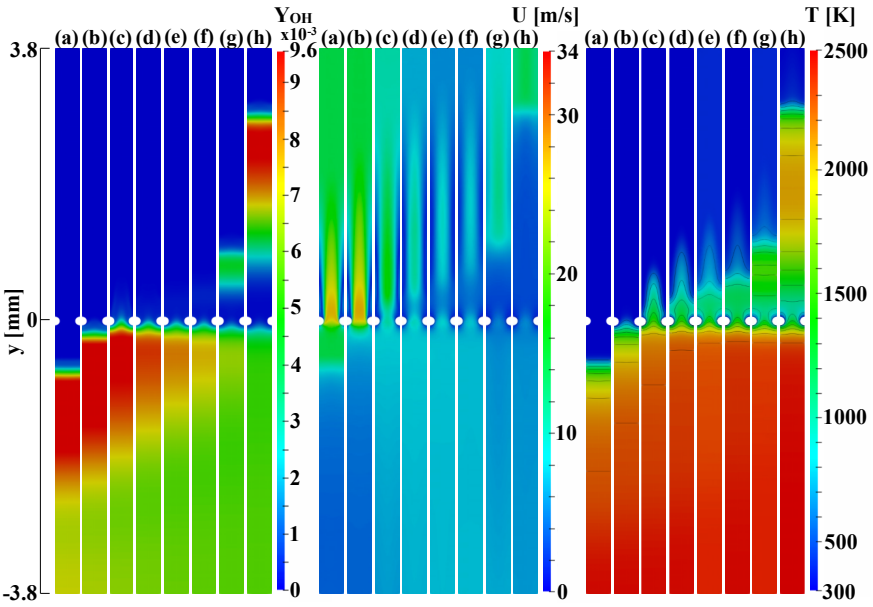

Figure 5: Near-critical case, mesh spacing $L = 0.2$ mm. Times relative to flame arrival at the wire location are a) -30 μs, b) 0 μs, c) +30 μs, d) +60 μs, e) +90 μs, f) +120 μs, g) +180 μs, h) +300 μs,

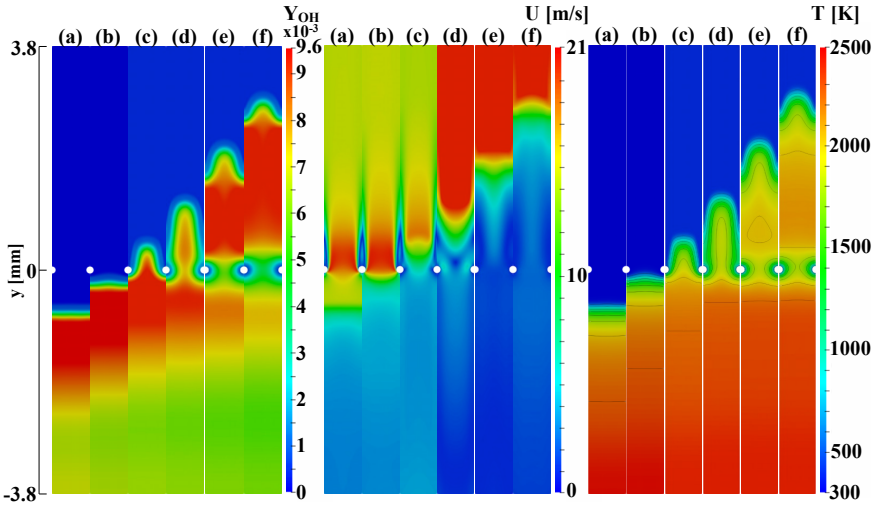

Figure 6: Super-critical case, mesh spacing $L = 0.5$ mm. Times relative to flame arrival at the wire location are a) -30 μs, b) 0 μs, c) +30 μs, d) +60 μs, e) +90 μs, c) +120 μs.

3.2 Péclet Number

A standard nondimensional representation of critical arrestor dimensions is to compute a Péclet number $Pe = UL/\alpha$ based on a reference velocity U and thermal diffusivity $\alpha = k/\rho C_p$ of the gas. In studies of flame-wall interactions [1], an alternative definition is used, $Pe = \delta_Q/\delta$, where δ_Q is a measured distance at which flame quenching is observed to occur and δ is a reference length scale. The length scale is either the notional flame thickness $\delta_S = \alpha/S_\ell^o$ with unburned gas properties used to define α or else the flame thickness δ_T based on the temperature profile and maximum slope.

Flame arrestors are frequently characterized by a critical value Pe^* and flames are quenched if $Pe < Pe^*$.

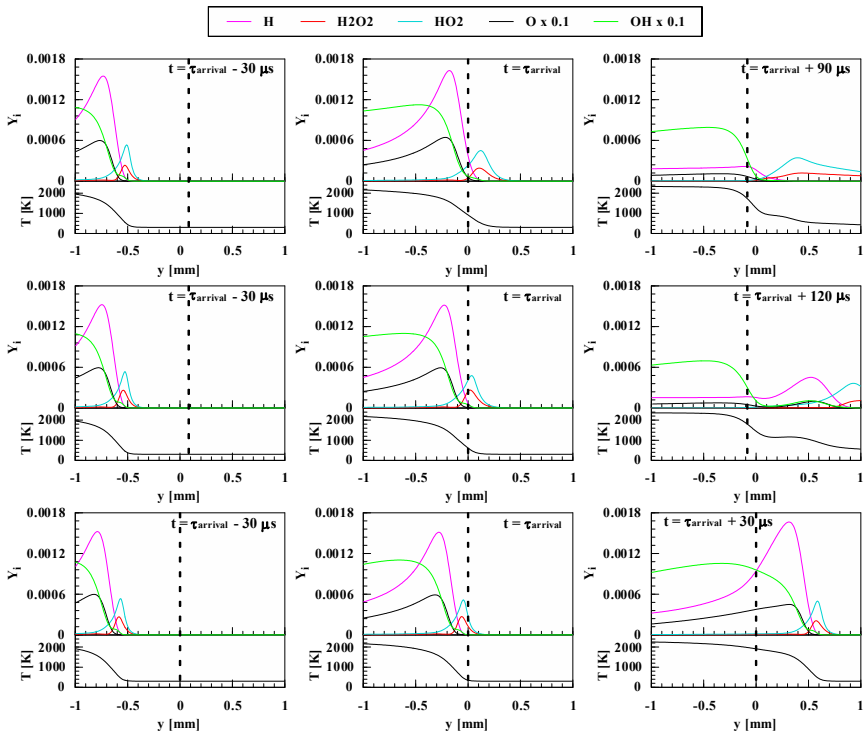

Figure 7: Species spatial profiles on the centerline (top: $L = 0.14$ mm, middle: $L = 0.2$ mm, bottom: $L = 0.5$ mm) at three times relative to flame arrival at the wire location.

Because there are such a wide range of arrestor designs and flame-wall interaction configurations (head-on, side-wall, crevice, etc), the critical value Pe^* is not universal and values between 1 to 100 are reported for various situations. The values for flame-wall interaction are not directly applicable to flame arrestors because of the importance of processes downstream of the arrestor element (Fig. 5) and the distinction between L and δ_Q. We have analyzed our results in terms of Péclet number defined as $Pe = L/\delta_S$. The values as function of Φ are shown in Fig. 8 with the interpolated critical condition Pe^* shown as a smooth curve increasing with increasing equivalence ratio from 2.5 at $\Phi = 0.4$ to 15 at $\Phi = 1.6$. These values and the trend are commensurate with past studies on flame arrestors.

4 Conclusions

The results of our simulations demonstrate the potential of using numerical simulation to investigate flame arrestors. Our results are for a very simplified geometry (multiple mesh layers are used in actual applications) but illustrate the key features of the flame-arrestor interaction. We have identified three regimes from our simulations that characterize the interaction and role of thermal conduction in the success or failure in extinguishing the flame. Near the surface of the wires in the mesh, the flame is always quenched within the cold portions of the thermal boundary layer. The extent of the penetration of the thermal layer into central region of the flow between the wires determines how much of the flame is extinguished and the subsequent evolution as the hot products and any remaining flame surface propagate downstream. For a given mixture and wire diameter, we find that there is a definite wire spacing L^* that separates the supercritical regime ($L > L^*$), which is characterized by flame transmission, from the subcritical regime ($L < L^*$), which is characterized by the flame being extinguished. The near-critical regime with $L \approx L^*$ is of particular interest and demonstrates that even when the flame is locally extinguished near the arrestor, reestablishment of a propagating flame can occur downstream if continued reaction within the hot products is able to regenerate enough radicals to restart the coupled chain-branching/energy release process essential

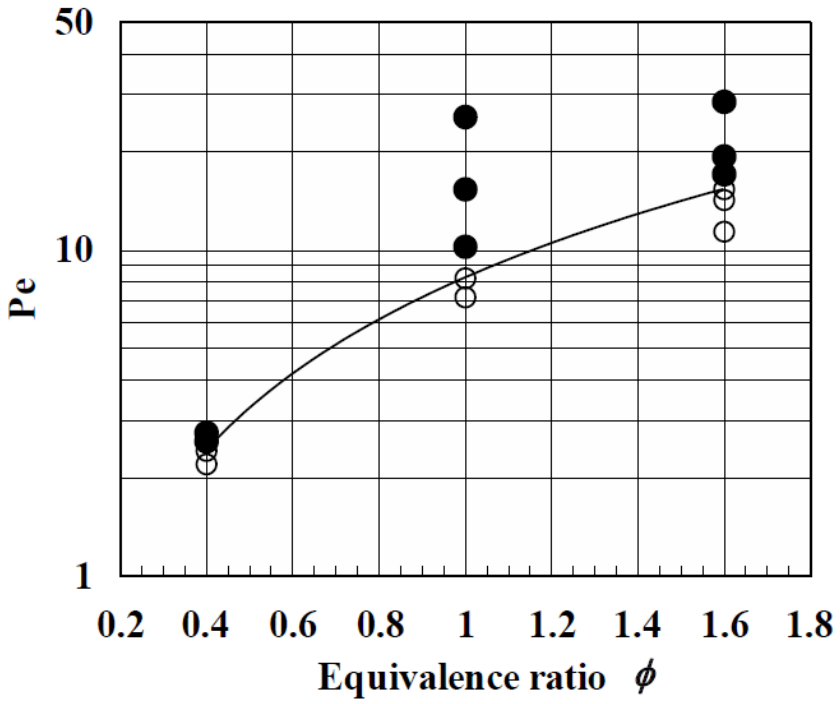

Figure 8: Péclet number analysis of simulation results shown in Fig. 3.

to flame propagation. The significance of this for future studies is that applications to fuels other than hydrogen and complex geometries at industrial scale (e.g., flame arrestors in large pipelines) will face the challenge of chemical model reduction that will faithfully model reactions networks with multiple pathways for numerous radical species and reactive intermediates.

Acknowledgments

This study was supported by The Boeing Company (CT-BA-GTA-1) and computing resources were provided by the Extreme Science and Engineering Discovery Environment (XSEDE), NSF grant ACI-1053575. HS was supported by a fellowship from the Shibaura Institute of Technology.

References

[1] A. Dreizler and B. Bohm. Advanced laser diagnostics for an improved understanding of premixed flame-wall interactions. *Proc. Combustion Inst.*, 35:37–64, 2015. 1, 7

[2] D. Goodwin, H. Moffat, and R. Speth. Cantera: an object-oriented software toolkit for chemical kinetics, thermodynamics, and transport processes. www.cantera.org, 2017. 3

[3] S. Grossel. *Deflagration and Detonation Flame Arresters.* Center for Chemical Process Safety of the American Institute of Chemical Engineers, New York, NY USA, 2002. 1, 2, 5

[4] ISO. Flame Arresters – Performance Requirements, Test Method and Limits for Use. International Standard ISO 16852:2008(E), International Organization for Standardization, 2008. 1

[5] T. Kim, D. Lee, and S. Kwon. Effects of thermal and chemical surface–flame in- teraction on flame quenching,. *Combust. Flame*, 146:19–28, 2006. 2

[6] B. Lewis and G. von Elbe. *Combustion, Flame and Explosions of Gases*. Academic Press, New York, NY USA, 2nd edition, 1961. 3, 5

[7] D. Lietze. Crimped metal ribbon flame arrestors for the protection of gas measurement systems. *J. Loss Prevention in the Process Industries*, 15(2):29–35, 2002. 5

[8] R. Mari, B. Cuenot, J.-P. Rocchi, L. Selle, and F. Duchaine. Effect of pressure on hydrogen/oxygen coupled flame–wall interaction. *Combust. Flame*, 168:409–419, 2017. 2

[9] J. Melguizo-Gavilanes, S. Boeck, R. Mevel, and J. Shepherd. Hot surface ignition of stoichiometric hydrogen-air mixtures. *J. Hydrogen Energ.*, 42(11):7393–7403, 2017. 2, 4

[10] J. Melguizo-Gavilanes, R. Mevel, S. Coronel, and J. Shepherd. Effects of differential diffusion on ignition of stoichiometric hydrogen-air by moving hot spheres. *Proc. Combustion Inst.*, 36:1155–63, 2017. 2

[11] R. Mevel, S. Javoy, F. Lafosse, N. Chaumeix, G. Dupre, and C.-E. Paillard. Hydrogen–nitrous oxide delay times: Shock tube experimental study and kinetic modelling. *Proc. Combustion Inst.*, 32:359–266, 2009. 2

[12] H. Saitoh, T. Otsuka, and N. Yoshikawa. Quenching evaluation of flame arresters for a damage mitigation system against hydrogen explosions in nuclear power plants. In *The 27th International Symposium on Transport Phenomena 2016*, Honolulu, HI USA, Sept. 2016. ISTP27-111. 1, 2

[13] H. Weller, G. Tabor, H. Jasak, and C. Fureby. A tensorial approach to computational continuum mechanics using object-oriented techniques. *Computers in Physics*, 12(6):620–631, 1998. 2